



Universiteit
Leiden
The Netherlands

Two-dimensional optics : diffraction and dispersion of surface plasmons

Chimento, P.F.

Citation

Chimento, P. F. (2013, May 22). *Two-dimensional optics : diffraction and dispersion of surface plasmons*. Retrieved from <https://hdl.handle.net/1887/20901>

Version: Not Applicable (or Unknown)

License: [Leiden University Non-exclusive license](#)

Downloaded from: <https://hdl.handle.net/1887/20901>

Note: To cite this publication please use the final published version (if applicable).

Cover Page



Universiteit Leiden



The handle <http://hdl.handle.net/1887/20901> holds various files of this Leiden University dissertation.

Author: Chimento, Philip

Title: Two-dimensional optics : diffraction and dispersion of surface plasmons

Issue Date: 2013-05-22

6

Anomalous dispersion of surface plasmons

We demonstrate, using surface plasmon resonance experiments in the Kretschmann and Otto configurations, a region of anomalous dispersion in the effective mode index of surface plasmons on aluminum in the near-infrared. This phenomenon is a consequence of aluminum's parallel-band transition at 1.5 eV. Our results show that the transition is only weakly present in aluminum layers of the order of 10 nm.

6.1 Introduction

RADIATIVE AND DISSIPATIVE LOSSES PLAY an important role in the field of plasmonics. While radiative loss is commonly considered useful, providing the coupling mechanism to the outside world, dissipative loss does not have this positive side. Apart from the drive towards lossless plasmonics,¹ the usual response to this challenge involves the use of materials, in this case metals, that have minimal dissipation.² Often, the metals that have low loss at optical frequencies have dielectric properties that exhibit Drude-like dispersion, that is, the dielectric properties are dominated by intraband electronic transitions. The Drude-like behavior implies that the dispersion of the effective surface plasmon mode index n_{SP} is always normal, i.e.:

$$\frac{dn_{\text{SP}}}{d\lambda} < 0 \text{ and } \frac{d^2n_{\text{SP}}}{d\lambda^2} > 0. \quad (6.1)$$

Anomalous dispersion in bulk materials such as atomic vapors is usually associated with a resonance in the absorption; there the vapor is essentially opaque so that the dispersion is usually difficult to measure directly.³ A discussion of the dispersive properties of a surface plasmon is

¹ Berini and De Leon, 2012.

² West et al., 2010.

³ King, 1917.

slightly more involved because a surface plasmon is a mode and therefore it is the *modal dispersion* that we probe. Moreover, in a simple geometry, it is a mode that propagates along the interface between two materials and therefore it probes the dispersion of *both* materials. In quite a few experiments the surface plasmon field extends into a number of layers with different dielectric properties, and the anomalous dispersion can arise as a consequence of the dispersive properties of each material separately, or combined. For example, the dispersion relation of the surface plasmon can be influenced by interaction with a dye monolayer.⁴ Here we address the simple case that the anomalous dispersion of a surface plasmon is caused by the dispersive properties of the metal, and not of the other materials into which it extends. Even in this simple case, the answer will turn out to depend on the experimental approach chosen.

⁴ Wähling, 1981.

Following the reasoning of the previous paragraph, we are searching for a plasmonic material — i.e. a metal where surface plasmons are not damped too strongly — which exhibits a relatively narrow peak in the imaginary part of the dielectric constant, and thus in the bulk absorption. Actually, there are quite a few metals that exhibit a resonance of this kind, such as aluminum,⁵ magnesium⁶ and calcium,⁷ to name just a few. For these metals, the spectral band associated with the extra absorption is known as parallel-band absorption:⁸ the absorption arises as a consequence of an interband transition between parallel electronic bands near the Fermi energy. From an experimental point of view, aluminum is attractive since it is a metal that has wide applications in both optics and plasmonics. Moreover, compared to the other materials mentioned above, it is quite easily handled.

⁵ Ehrenreich, Philipp, and Segall, 1963.

⁶ Mathewson and Myers, 1973.

⁷ Hunderi, 1976.

⁸ Harrison, 1966.

The parallel-band absorption in aluminum is quite well known among optics experts as it is the effect underlying the small dip at $\lambda \approx 800$ nm ($\hbar\omega \approx 1.5$ eV) in the reflectance of aluminum, and thus of all aluminum mirrors.⁹ Ehrenreich et al.¹⁰ were first in explaining this dip as the result of a parallel-band transition. Their analysis of the optical properties of aluminum was extended and refined by Harrison¹¹ and Brust.¹² Almost a decade later, their model of the optical properties of aluminum, as a weakly perturbed free-electron metal,¹³ was further refined by Ashcroft and Sturm¹⁴ resulting in explicit expressions for the optical conductivity, which were shown to agree well with experimental data.

⁹ Strong, 1936; Bennett et al., 1963.

¹⁰ Ehrenreich et al., 1963.

¹¹ Harrison, 1966.

¹² Brust, 1970.

¹³ Harrison, 1966.

¹⁴ Ashcroft and Sturm, 1971.

In this chapter, we investigate the optical dispersion of surface plasmons traveling on a metallic aluminum interface in the spectral region of parallel-band absorption, using attenuated total reflection in the Kretschmann and Otto configurations.

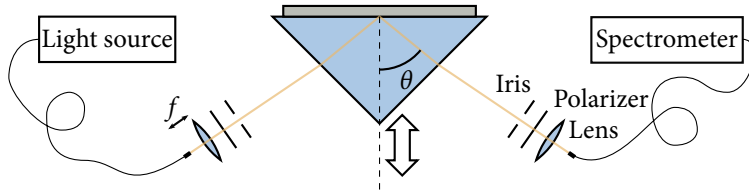


Figure 6.1: Sketch of the experimental setup. The setup is placed on a pair of rotation stages so that for a certain desired internal angle of incidence θ , the light source and detector are rotated to the correct angles. The prism is also placed on a translation stage aligned with the prism's axis of symmetry, so that the setup remains symmetric and the beam always probes the same spot on the coated face.

6.2 Experiment

THE LOCATION OF THE PARALLEL-BAND FEATURE in the spectrum suggests that in our search for plasmonic anomalous dispersion we need to study the spectral region between roughly 600 and 1000 nm. For the experiment this implies the use of a broadband light source such as a lamp, which, typically, has low spectral brightness. For this reason we choose to couple with the surface plasmon by traditional attenuated total reflection methods, as originally proposed by Kretschmann and Otto. The method put forward by Kretschmann¹⁵ is almost universally considered preferable to that of Otto;¹⁶ but in the present case the Otto configuration has some very strong advantages, as discussed in chapter 5. It was successfully used by Tillin and Sambles¹⁷ to measure the dielectric function of aluminum. Here we will present experimental results for both configurations and we will see that the results are quite different, reflecting the fact that the two distinct experiments probe an entirely different surface plasmon mode.

Figure 6.1 shows the generic experimental setup. Highly collimated p -polarized white light from a fiber-coupled tungsten halogen lamp (Ocean Optics HL-2000-HP-FHSA) is incident on one of the faces of a prism; the collimated beam that is internally reflected off the metal-covered face leaves the prism through its third face and is collected on the input facet of a fiber-coupled mini-spectrometer (Ocean Optics USB2000). During the experiment we rotate the prism in steps that increase the internal angle of incidence by 0.05° ; the mini-spectrometer with the associated optics is mounted on an arm that co-rotates with the prism so that it catches the reflected beam. In order to ensure that we always probe the same spot on the aluminum layer, we adjust the prism's position after each rotation step. For each orientation of the prism we measure the reflected spectrum.

FOR THE KRETSCHMANN EXPERIMENT, we used a right-angled BK7 glass prism, with broadband near-infrared antireflection coatings (650–950 nm) on the two faces adjacent to the right angle. On the hypotenuse we deposited a thin layer of aluminum, using a Leybold Heraeus z400

¹⁵ Kretschmann, 1971.

¹⁶ Otto, 1968.

¹⁷ Tillin and Sambles, 1988.

sputtering system. To prevent oxidation of the metal film, we used the same sputtering system to immediately cap it with a Si_3N_4 layer of a few nanometers thickness. The critical angle for total internal reflection on the BK7–air interface is around 41.5° , slightly less than 45° , meaning that the beam is almost normally incident on the antireflection-coated entrance and exit faces.

In the Kretschmann configuration, the surface plasmon that can be excited by the attenuated total reflection technique resides on the Si_3N_4 -capped outer surface of the aluminum film. Because of the high optical loss in bulk aluminum, the calculated layer thickness that yields critical coupling is approximately 6 to 10 nm in the spectral region we are studying.

However, thin aluminum films have optical properties quite different from those of bulk aluminum.¹⁸ In the measurements of Novotny et al.,¹⁹ the parallel band resonance is not even in evidence for layers thinner than 9 nm, supposedly because the electron scattering length is then of the same order of magnitude as the layer thickness. In order to find the best layer thickness for critical coupling, we performed experiments on aluminum layers of several different thicknesses. The results here are shown for a prism coated with a 10.8 ± 0.6 nm thick aluminum layer with 7.6 ± 0.3 nm Si_3N_4 on top. We illustrate the layer stack on the prism and the plasmonic mode we probe in Fig. 6.2. Figure 6.3 shows experimental results for this prism for a number of representative wavelengths.

The most striking feature of the experimental results is that the reflectance is relatively small for a wide range of angles of incidence and seems not to recover at large angles, quite in contrast to the well-known case of surface plasmons on gold or silver films. As discussed in the previous chapter, this is typical for a metal where the ratio of the imaginary and real parts of the dielectric constant $|\epsilon''/\epsilon'|$ is of order 1.

FOR THE OTTO EXPERIMENT, we used an equilateral prism made of F2 glass ($n \approx 1.608$ at 800 nm), again with coatings deposited on all three faces: broadband near-infrared antireflection coatings ($R < 2\%$ for 500–940 nm) on the two faces through which light enters and exits the prism; and a compound layer on the third side consisting of 570 nm MgF_2 (the low-index dielectric), 100 nm aluminum, and 110 nm SiO_2 as a capping layer to prevent oxidation. For this prism, the critical angle for total internal reflection at the F2– MgF_2 interface is around 59° , depending on wavelength. Again, the light beam is almost normally incident on this prism's antireflection-coated faces.

¹⁸ Du et al., 2006; Novotny, Bulir, Lancok, Pokorný, and Bodnar, 2011.

¹⁹ Novotny, Bulir, et al., 2011.

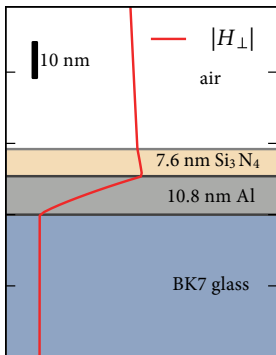


Figure 6.2: Schematic of the various layers deposited on the BK7 prism used in the Kretschmann setup. The calculated amplitude of the magnetic component of the surface plasmon field H_{\perp} is shown in red. The left edge of the figure corresponds to zero amplitude. The field mode decays exponentially into the glass and air with decay lengths of $9.1 \mu\text{m}$ and $0.76 \mu\text{m}$, respectively. Hence, the decay is not visible at this scale.

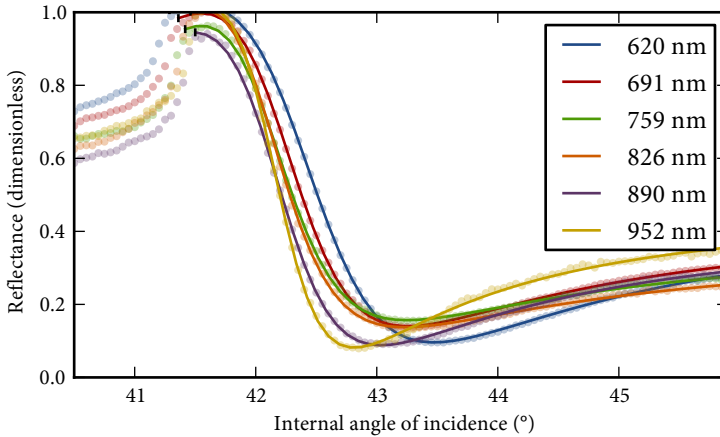


Figure 6.3: Experimental results for the angle-dependent reflectance for several representative wavelengths, measured using the Kretschmann configuration and the sample illustrated in Fig. 6.2. The dots indicate measured values, and the solid lines are fits to the data using (6.2), discussed later in this chapter. The fits cut off at the critical angle for total internal reflection from BK7 glass to air, as indicated by the small black markers.

For our experiments we chose a MgF_2 spacer layer of 570 nm thickness. Theoretically, we expect this layer to provide critical coupling in the 750–850 nm wavelength range. Note that in this setup we excite the surface plasmon at the interface between the aluminum film and the MgF_2 layer. In contrast to the case of the Kretschmann configuration, the metallic layer is sufficiently thick that it may be considered to be bulk aluminium.

Experimental results for the reflectance as a function of internal angle for the Otto setup are shown in Fig. 6.5, for a number of representative wavelengths across the wavelength range of interest. The reflectance curves are narrower than in the Kretschmann configuration, but for the longer wavelengths the coupling is far from critical.

6.3 Results and interpretation

FROM THE EXPERIMENTAL RESULTS, as shown in Figs. 6.3 and 6.5, we extract the resonance angle, i.e. angular position of the minimum of the reflectance curves. We plot the resonance angle for both configurations as a function of wavelength in Fig. 6.6.

The first thing to notice is that the two curves are quite similar qualitatively. In both cases, the resonance angle decreases as a function of wavelength at the shorter and longer wavelengths measured, while at intermediate wavelengths the resonance angle goes through a local maximum. In the Kretschmann configuration, the maximum is less pronounced than in the Otto configuration. More careful inspection of the data brings

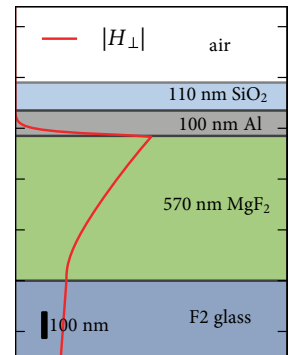
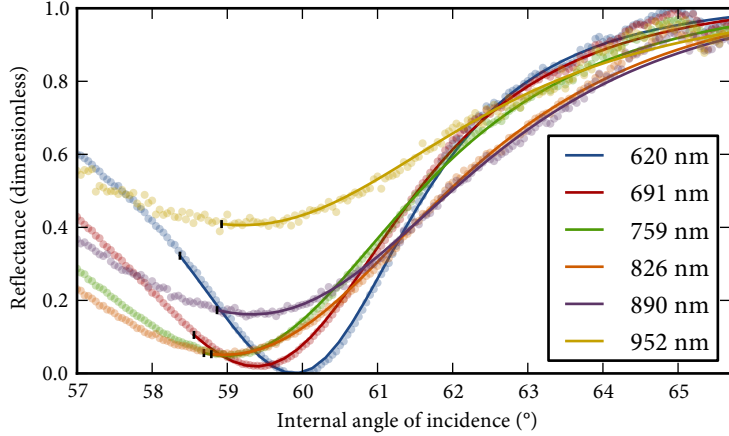


Figure 6.4: Illustration of the various layers deposited on the F_2 prism used in the Otto setup. The calculated amplitude of the magnetic field H_{\perp} associated with the surface plasmon mode is shown in red, in order to illustrate the plasmonic mode that we are probing in this experiment. The left edge of the figure corresponds to zero amplitude.

Figure 6.5: Example reflectance curves for several representative wavelengths, measured using the Otto configuration and the sample illustrated in Fig. 6.4. The dots indicate measured values, and the solid lines are fits to the data using (6.2), discussed later in this chapter. The fits cut off at the critical angle for total internal reflection from F2 glass to MgF₂, as indicated by the small black markers.



out the differences: in the Kretschmann setup the maximum lies somewhere between 800 and 850 nm, while the Otto data exhibit a maximum near 900 nm. Note that the Kretschmann data are noisier than the Otto data; this reflects the very broad minimum of the experimental reflectance curves for the Kretschmann configuration, the exact position of which is somewhat difficult to determine, in particular when the signal to noise ratio is not good, as is to be expected in a reflectance minimum. The Otto curves exhibit a much narrower dip, the center of which is therefore easier to determine. At longer wavelengths ($\lambda > 900$ nm) the angular reflectance spectra in the Otto configuration also exhibit a shallow dip, as our experimental system is far from critical coupling there. The difficulty in finding the minimum of these shallow curves is reflected in the noise in Fig. 6.5.

IT IS TEMPTING to draw the conclusion from the data of Fig. 6.6 that the surface plasmon modes in the Kretschmann and Otto configurations exhibit anomalous dispersion. However, the resonance angle is not a good measure for the surface plasmon wave vector, as discussed in chapter 5. In order to analyze the data properly, obtaining both the real and imaginary parts of the surface plasmon mode index, we fit the reflectance curve above the critical angle with the Fano-type lineshape (5.15, 6.2), for each wavelength studied. As shown in chapter 5, this lineshape is an excellent description of the surface plasmon resonance curves for angles of incidence above the critical angle.

$$R(k_x) = \left| B + \frac{A e^{i\phi} k_{SP}''}{k_{SP}' + i k_{SP}'' - k_x} \right|^2, \quad k_x > k_{cr}. \quad (6.2)$$

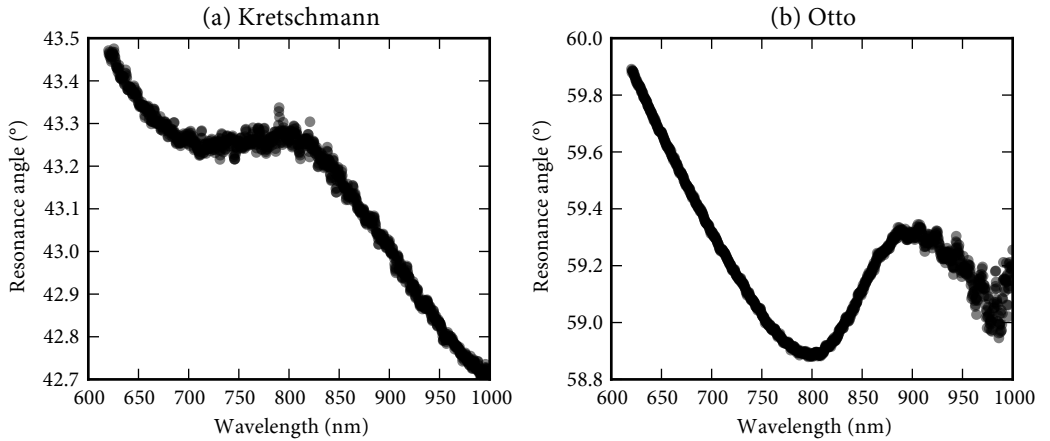


Figure 6.6: Measured resonance angle as a function of wavelength for the Kretschmann experiment (a) and the Otto experiment (b).

Here, R is the reflectance; A , B , ϕ , k'_{SP} , and k''_{SP} are fit parameters. The parameter B can be identified with the modulus of the reflection coefficient r_{01} at the first interface. Since we are only fitting the part of the curve above the critical angle, we can set $B = 1$ for the Otto configuration. From the complex-valued k_{SP} obtained in this way, we plot the real and imaginary parts of the surface plasmon mode index $n_{\text{SP}} = k_{\text{SP}}/k_0$ in Fig. 6.7.

For comparison, we show calculated curves for the respective layer systems using Sellmeier models for the dielectric functions of BK7 glass, F2 glass,²⁰ MgF_2 ,²¹ SiO_2 ,²² and Si_3N_4 .²³ We used Ashcroft and Sturm's model for the dielectric function²⁴ of the thin layer of aluminum in the Kretschmann experiment, with modified values for the electron scattering times, as discussed in chapter 7. We measured the dielectric function of the thin aluminum layer by ellipsometry and fit Ashcroft and Sturm's expression to these data, with the electron scattering times as variable parameters, yielding 9.7 fs for free electron scattering and 1.9 fs for parallel-band scattering. For the thicker aluminum used in the Otto experiment, we used a Drude-Lorentz model for the dielectric function²⁵ based on tabulated values.²⁶ These estimates exhibit good qualitative agreement with the behavior shown in Fig. 6.7.

The Ashcroft-Sturm expression reflects the parallel-band resonance's much heavier damping in the thinner layer; the electron scattering time is greatly reduced because the scattering length is of the same order as the layer thickness. Based on a Fermi velocity of 2.03×10^6 m/s,²⁷ a parallel-band scattering time of 3.8 fs in bulk aluminum²⁸ yields a mean free path of 7.7 nm, which is close enough to the layer thickness of 10.8 nm that

²⁰ Schott AG, 2012.

²¹ Dodge, 1984.

²² Malitson, 1965.

²³ Bååk, 1982.

²⁴ Ashcroft and Sturm, 1971.

²⁵ Rakić et al., 1998.

²⁶ Smith, Shiles, and Inokuti, 1985.

²⁷ Ashcroft and Mermin, 1976, p. 38.

²⁸ Mathewson and Myers, 1972.

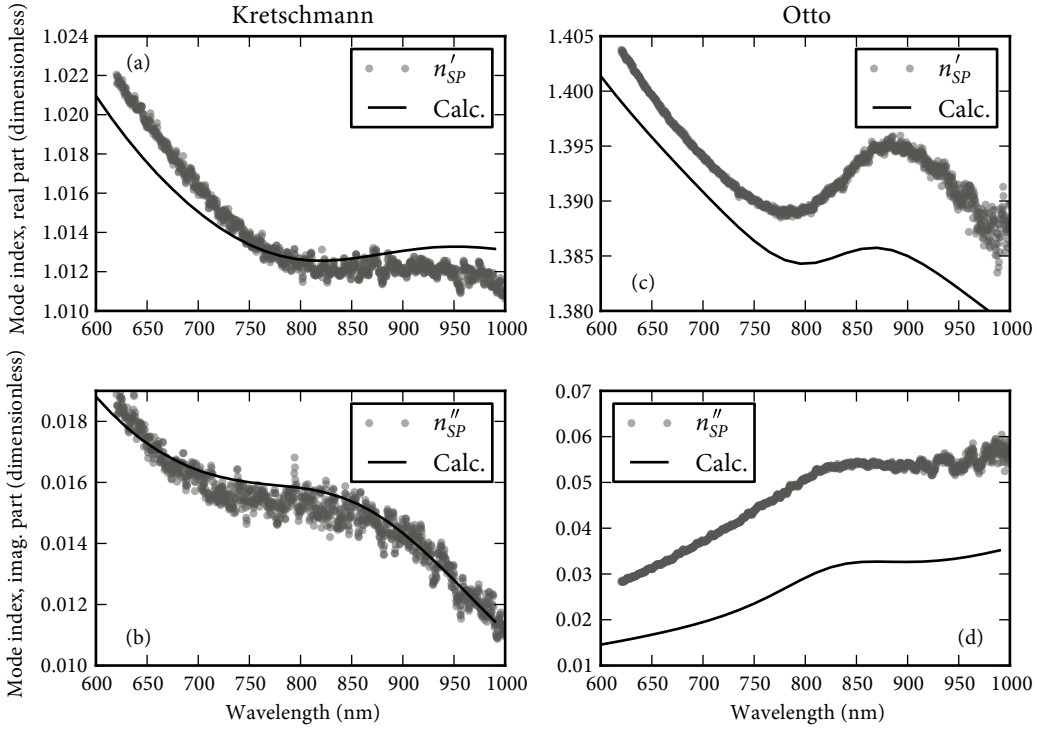


Figure 6.7: Real and imaginary parts of the surface plasmon mode index $n_{SP} = k_{SP}/k_0$ obtained from our measurements on aluminum films in the Kretschmann (a, b) and Otto (c, d) configurations, as a function of free-space wavelength. In (a) and (b), we also show calculated values for the mode index in the Kretschmann layer system, using expressions for the dielectric constant of aluminum as given by Ashcroft and Sturm (1971). In (c) and (d), we show the calculated mode index in a similar manner, but using published values for the dielectric function of bulk aluminum metal.

surface scattering effects play more of a part. Our fitted value of 1.9 fs for the parallel-band scattering time, on the other hand, corresponds to a mean free path of 3.8 nm. In Figs. 6.7c–d, we compare the measured results to published values for bulk aluminum; however, in chapter 7 we will also demonstrate an improved correspondence by adjusting the scattering times.

Figure 6.7 brings out a few aspects quite clearly: for both the Kretschmann and Otto configuration, there is a wavelength region where the dispersion of the modal index of the surface plasmon is identifiably anomalous. However, the dispersion for the two configurations is quite different, reflecting the large difference of the surface plasmon’s modal profile in the two cases studied. One reason is that the ‘Otto plasmon’ resides largely on the interface between MgF_2 and aluminum, whereas the mode in the Kretschmann configuration essentially has the character of an aluminum-air surface plasmon. Our Otto plasmon is therefore much more ‘metallic’ than our Kretschmann plasmon; the former is a better vehicle for prob-

ing the metal's material dispersion. A second reason that may play an important role in explaining the difference between the dispersion of the two modes is the effect of metal film thickness. The Kretschmann plasmon resides on an aluminum layer so thin that its optical properties seem to be quite different from those of bulk metallic aluminum. In the Otto setup, the film is sufficiently thick that its behavior is closer to that of bulk metal.

Another difference apparent from the figure is that the modal loss is much smaller for the Kretschmann plasmon than for its Otto counterpart. This difference can also be attributed to the Otto plasmon being considerably more metallic.

6.4 Conclusion

WE HAVE DEMONSTRATED ANOMALOUS DISPERSION in the effective mode index of surface plasmons on metallic aluminum layers, paired with air in the Kretschmann configuration and MgF_2 in the Otto configuration. The anomalous dispersion is a direct consequence of aluminum's optical properties, and not those of the dielectric: specifically, the absorption due to aluminum's interband transition at 1.5 eV.

The surface plasmon modes we have measured are not, in either of the two configurations, the same as the simple surface plasmon mode on an infinite interface between two half-spaces. Each configuration has its own plasmonic mode with a slightly different mode index. We find that the properties of the 'Otto plasmon' have more in common with the metal than those of the 'Kretschmann plasmon,' which is situated more in the dielectric.

Our Kretschmann results suggest, by the weak anomalous dispersion, that aluminum's interband transition is only weakly present if the aluminum layer is thin enough. However, our Otto results show the stronger anomalous dispersion expected based on various models for the optical properties of aluminum.

Appendix 6.A Comparison of dielectric functions obtained by reflection and ellipsometry

IN ORDER TO CHECK THE CONSISTENCY of our results, we also analyzed the Kretschmann reflection curves using the entire Fabry-Perot expression for reflection, $R = |r_{0123}|^2$, with the real and imaginary parts of ε_1 , the dielectric function of the aluminum layer, as fit parameters. We used the layer thicknesses obtained by ellipsometry, and Sellmeier models for the dielectric functions of BK7²⁹ and Si_3N_4 .³⁰ Figure 6.8 shows the aluminum dielectric function we obtained in this way, compared to the aluminum dielectric function we obtained by ellipsometry.

²⁹ Schott AG, 2012.

³⁰ Bååk, 1982.

We conclude that the methods are in excellent agreement about the real part of the dielectric function, but that the Kretschmann measurement has a tendency to overestimate the imaginary part compared to the ellipsometric measurement.

Figure 6.8: Dielectric function of our 10.8 nm layer of aluminum, measured by ellipsometry (green, negative real part, and orange, imaginary part) and Kretschmann reflectance (blue, negative real part, and red, imaginary part). The shaded areas indicate the confidence interval output by the ellipsometer's fitting routine.

